ELSEVIER

Nuclear Physics B 511 (1998) 451–478

NUCLEAR PHYSICS B

Classical approximation for time-dependent quantum field theory: Diagrammatic analysis for hot scalar fields

Gert Aarts [a,1], Jan Smit [a,b,2]

[a] *Institute for Theoretical Physics, Utrecht University, Princetonplein 5, 3508 TA Utrecht, The Netherlands*
[b] *Institute for Theoretical Physics, University of Amsterdam, Valckenierstraat 65, 1018 XE Amsterdam, The Netherlands*

Received 16 July 1997; accepted 23 October 1997

Abstract

We study time-dependent correlation functions in hot quantum and classical field theory for the $\lambda\phi^4$ case. We set up the classical analogue of thermal field theory and make a direct comparison between the quantum and classical diagrams. A restriction to time-independent correlation functions gives the connection with conventional dimensional reduction. If the parameters in the classical theory are chosen according to the dimensional reduction matching relations, the classical expressions are cutoff independent and they approximate the quantum expressions, provided that the external momenta and frequencies are small with respect to the temperature. © 1998 Elsevier Science B.V.

PACS: 11.10.Wx; 11.10.Gh; 11.15.Kc
Keywords: Real-time quantum field theory at finite temperature; Classical approximation

1. Introduction

Time-dependent phenomena in hot relativistic quantum field theory play an important role in cosmology (baryogenesis, inflation) and heavy-ion collisions. Non-perturbative calculations of these phenomena under general circumstances are very difficult. A potentially powerful approach is the classical approximation, in combination with numerical simulations. When this approach was introduced for the computation of the rate

[1] E-mail: aarts@fys.ruu.nl
[2] E-mail: jsmit@phys.uva.nl

PII S0550-3213(97)00723-2

of sphaleron transitions [1,2], the idea was to choose the cutoff of the order of the temperature, since only the low momentum modes of the fields are expected to behave classically at high temperature. This raises the question how the results of the simulations depend on the cutoff. Improving the method by consistently taking the high momentum modes into account (by integrating them out of the original quantum theory [3,4]) leads to very complicated effective equations of motions [5,6].

To try to get around these problems we investigated in [7] the effect of taking the momentum cutoff to infinity, in hot time-dependent *classical* $\lambda\phi^4$ theory. It turned out that the cutoff dependence could simply be cancelled with local counterterms, as in the dimensional reduction approach for time-independent quantities. Furthermore we found that with a suitable choice of the parameters in the classical hamiltonian, the classical plasmon damping rate is the leading order (in λ) result of the quantum theory. This result has been confirmed in a recent calculation [8].

In this paper we give a diagrammatic comparison between the real-time correlation functions in the quantum theory and the classical theory for $\lambda\phi^4$. We show that there is a direct correspondence between quantum and classical diagrams, and that the classical result is the leading order quantum result at high T, provided that the classical parameters are chosen correctly, and the theory is weakly coupled.

After a short review of the dimensional reduction approach for time-independent correlation functions, we introduce a version of the real-time formalism for finite-temperature quantum field theory which is appropriate for a direct comparison with the classical theory. We then introduce the classical approximation and show how to identify diagrams that arise in perturbation theory. After this setup, we calculate the two-point function to two loops and the four-point function to one loop, and compare the quantum with the classical results. Throughout we work with $\hbar = 1$, except when we explicitly want to indicate what part of the results is really classical and what part is quantum.

2. Dimensional reduction for time-independent quantities

We start with a brief summary of the dimensional reduction approach for time-independent quantities, see for example, Refs. [9–11].

Static quantities in a quantum field theory at finite temperature are most easily calculated in the imaginary time or Matsubara formalism [12]. The partition function is given by

$$Z = \int \mathcal{D}\phi\, e^{-S_E},$$

with the euclidean action

$$S_E = \int_0^\beta d\tau \left[\int d^3x \left(\tfrac{1}{2}(\partial_\tau \phi)^2 + \mathrm{ct} \right) + \bar{V}(\phi) \right], \tag{2.1}$$

where $\bar{V}$ is the potential energy

$$\bar{V}(\phi) = \int d^3x \left(\frac{1}{2}(\nabla\phi)^2 + \frac{1}{2}\bar{m}^2\phi^2 + \frac{\bar{\lambda}}{4!}\phi^4 \right),$$

and ct denotes the counterterms. We assume dimensional renormalization in the $\overline{\rm MS}$ scheme and $\bar{m}$ and $\bar{\lambda}$ are the corresponding parameters. The counterterms are given in Appendix A. The field satisfies periodic boundary conditions $\phi(\boldsymbol{x},0) = \phi(\boldsymbol{x},\beta)$, which leads to the decomposition

$$\phi(\boldsymbol{x},\tau) = T\sum_n e^{i\omega_n\tau}\phi_n(\boldsymbol{x}),$$

where $\omega_n = 2\pi nT$ are the Matsubara frequencies. In the dimensional reduction approach, an effective theory is constructed for ϕ_0. This effective theory is chosen to have the same form as the ϕ_0 part of the full quantum theory, but with effective parameters. Hence the partition function for the dimensionally reduced theory is given by

$$Z_{\rm DR} = \int \mathcal{D}\phi_0\, e^{-\beta V}, \tag{2.2}$$

with

$$V = \int d^3x \left(\frac{1}{2}(\nabla\phi_0)^2 + \frac{1}{2}\nu^2\phi_0^2 + \frac{\lambda}{4!}\phi_0^4 + \epsilon \right).$$

We did not absorb the prefactor β in the field and coupling constant as is usually done. For completeness we included an effective cosmological constant ϵ.

The parameters in the effective theory are determined by perturbatively matching correlation functions in the effective theory to correlation functions in the full theory. The effective theory needs regularization and we use a momentum cutoff Λ. Because it is super-renormalizable, only the effective mass parameter and the cosmological constant receive a Λ-dependent part. The divergent integrals appearing in the scalar field self-energy corresponding to the one-loop leaf diagram and the two-loop setting sun diagram are

$$\frac{\lambda T}{2}\int_{|\boldsymbol{k}|<\Lambda} \frac{d^3k}{(2\pi)^3}\frac{1}{\omega_k^2} = \lambda T\left(\frac{\Lambda}{4\pi^2} - \frac{m}{8\pi}\right),$$

$$-\frac{\lambda^2T^2}{6}\int_{|\boldsymbol{k}_{1,2,3}<\Lambda|} d\Phi_{123}(\boldsymbol{0})\frac{8}{\omega_{k_1}\omega_{k_2}\omega_{k_3}} = -\lambda^2T^2\left(\frac{1}{16\pi^2}\log\frac{\Lambda}{3m} + L_0\right), \tag{2.3}$$

where

$$\omega_k = \sqrt{\boldsymbol{k}^2 + m^2}, \tag{2.4}$$

$$d\Phi_{123}(\boldsymbol{p}) = \frac{d^3k_1}{(2\pi)^3 2\omega_{k_1}}\frac{d^3k_2}{(2\pi)^3 2\omega_{k_2}}\frac{d^3k_3}{(2\pi)^3 2\omega_{k_3}}(2\pi)^3\delta(\boldsymbol{p}-\boldsymbol{k}_1-\boldsymbol{k}_2-\boldsymbol{k}_3). \tag{2.5}$$

The regularization-dependent constant $L_0 = 0.0067$ [11]. The result of matching the two-point function [9] to two loops can be written in the form

$$\nu^2 = m^2 - \delta m^2, \qquad \delta m^2 = \lambda m_1^2 + \lambda^2 m_2^2, \tag{2.6}$$

with[3]

$$m^2 = \bar{m}^2 + m_{\rm th}^2, \qquad m_{\rm th}^2 = \frac{\bar{\lambda} T^2}{24}, \tag{2.7}$$

$$m_1^2 = \frac{\Lambda T}{4\pi^2} + \frac{m^2}{32\pi^2} \log \frac{\bar{\mu}^2}{\mu_T^2}, \qquad \mu_T \equiv 4\pi \exp(-\gamma_E) T, \tag{2.8}$$

$$m_2^2 = -T^2 \left(\frac{1}{16\pi^2} \left[\log \frac{\Lambda}{3T} - c - \frac{1}{2} \right] + L_0 \right), \tag{2.9}$$

Here $\bar{\mu}$ is the scale parameter in the $\overline{\rm MS}$ scheme and the constant $c = -0.34$ is given in [9,10]. For future convenience we have separated the effective mass parameter ν^2 into a tree level mass m^2, and two counterterms λm_1^2 and $\lambda^2 m_2^2$. The matching (2.9) is such that the three- and four-dimensional renormalized self-energies coincide at zero momentum.

For the coupling constant to one loop, the relation is

$$\lambda = \bar{\lambda} - \frac{3\bar{\lambda}^2}{32\pi^2} \log \frac{\bar{\mu}^2}{\mu_T^2}. \tag{2.10}$$

Finally for the cosmological constant, matched to one loop, we get

$$\epsilon = \bar{\epsilon} - \frac{\pi^2 T^4}{90} + \frac{m^2 T^2}{24} - \frac{m^4}{64\pi^2} \log \frac{\bar{\mu}^2}{\mu_T^2} - \frac{\Lambda^3 T}{6\pi^2} \left(\ln \frac{\Lambda}{T} - \frac{1}{3} \right) + \frac{\Lambda T m^2}{4\pi^2}. \tag{2.11}$$

Note that the Rayleigh–Jeans divergence in the energy density is cancelled, and the Stefan–Boltzmann law is put in by hand through the matching procedure.

Corrections to the dimensional reduction approximation are small when the thermal mass and external momenta are small compared to the temperature, i.e.

$$\frac{m_{\rm th}^2}{T^2} = \frac{\bar{\lambda}}{24} \ll 1, \qquad \frac{p^2}{T^2} \ll 1.$$

This is satisfied when the theory is weakly coupled and physical observables are dominated by momenta smaller than $\mathcal{O}(\sqrt{\lambda} T)$.

This completes the standard description of the dimensional reduction approach for time-independent quantities. In the following sections we move on to time-dependent correlation functions.

3. Real-time formulation of quantum field theory at finite temperature

In the preceding section we were only interested in static quantities. For this the imaginary-time formalism is very useful. However, to make a direct diagrammatic analysis of time-dependent correlation functions, a more suitable formulation is the real-time

[3] The choice here of the finite parts of $m_{1,2}^2$ differs from that in Ref. [7].

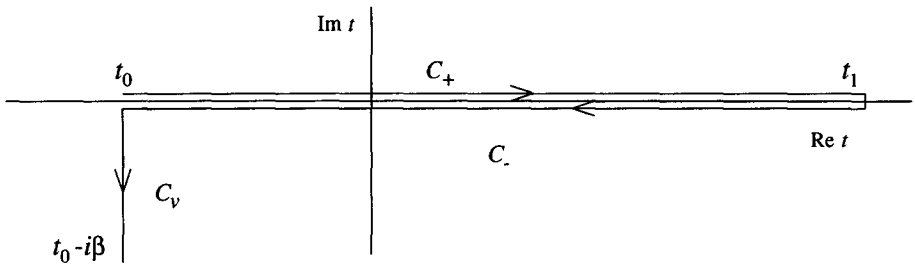

Fig. 1. Keldysh contour in the complex t-plane.

formalism [13,14]. In this section we review a version of the real-time formulation that is very convenient for a comparison with the classical theory.

The real-time expectation value

$$\langle O(t)\rangle = Z^{-1}\mathrm{Tr}\, e^{-\beta H} O(t), \tag{3.1}$$

with

$$Z = \mathrm{Tr}\, e^{-\beta H}, \qquad O(t) = e^{iHt} O e^{-iHt}$$

can be represented by the path integral

$$\langle O(t)\rangle = Z^{-1} \int \mathcal{D}\phi\, e^{iS} O(t),$$

with the action[4]

$$S = -\int_C dt \int d^3x \left(\frac{1}{2}\partial_\mu\phi\partial^\mu\phi + \frac{1}{2}\bar{m}^2\phi^2 + \frac{\bar{\lambda}}{4!}\phi^4 + \mathrm{ct} \right). \tag{3.2}$$

The subscript C labels the contour[5] in the complex t-plane shown in Fig. 1. The result is obviously independent of the initial and final times t_0 and t_1. In thermal field theory one lets $t_0 \to -\infty$ and $t_1 \to +\infty$. This leads to the introduction of two fields ϕ_+ and ϕ_- which live on the $+$ and $-$ branches of the contour. It has been shown [15,16] that the field on the vertical branch of the contour at $t_0 = -\infty$ can be ignored for the calculation of expectation values as in (3.1), such that in perturbation theory only the propagators and vertex functions for the $\pm$ field combinations enter. Explicitly, the vertex functions correspond to the interaction

$$-\int_{-\infty}^{\infty} dt \int d^3x \frac{\bar{\lambda}}{4!}(\phi_+^4 - \phi_-^4).$$

[4] We use a space-favoured metric $(-1,1,1,1)$; note in particular that $k^0 = -k_0$ corresponds to k^0 in the time-favoured metric $(1,-1,-1,-1)$.

[5] Other contours are also possible [13], but we prefer to use the Keldysh contour.

However, the form of the propagator for the $\pm$ fields reflects the vertical branch of the contour at $t_0 = -\infty$. For example, the full propagator for the $\pm$ fields is still given by the original operator representation ($t = x^0$),

$$
\begin{aligned}
G^{++}(x-x') &= \theta(t-t')G^{>}(x-x') + \theta(t'-t)G^{<}(x-x'),\\
G^{+-}(x-x') &= G^{<}(x-x'), \qquad G^{-+}(x-x') = G^{>}(x-x'),\\
G^{--}(x-x') &= \theta(t'-t)G^{>}(x-x') + \theta(t-t')G^{<}(x-x'),
\end{aligned}
$$

with

$$
G^{>}(x-x') = i\langle\phi(x)\phi(x')\rangle, \qquad G^{<}(x-x') = i\langle\phi(x')\phi(x)\rangle .
$$

These expectation values are related by the well-known KMS condition

$$
G^{>}(\boldsymbol{x}-\boldsymbol{x}', t-t') = G^{<}(\boldsymbol{x}-\boldsymbol{x}', t-t'+i\beta), \tag{3.3}
$$

which follows from the cyclicity of the trace and the fact that the time evolution and the canonical average are governed by the same hamiltonian. Using the KMS condition to determine the explicit form of the propagators takes into account the vertical branch [15,16]. We stress this point because we will follow the same steps when we consider the classical theory.

To make a direct relation with classical correlation functions, it is convenient to go to another basis, given by

$$
\begin{pmatrix} \phi_1 \\ \phi_2 \end{pmatrix} = \begin{pmatrix} (\phi_+ + \phi_-)/2 \\ \phi_+ - \phi_- \end{pmatrix} = R \begin{pmatrix} \phi_+ \\ \phi_- \end{pmatrix}, \tag{3.4}
$$

with

$$
R = \begin{pmatrix} 1/2 & 1/2 \\ 1 & -1 \end{pmatrix}.
$$

This is a variation of the Keldysh basis, where R is a rotation over $\pi/4$. In fact, the basis we use here is closely connected to the influence functional approach of Feynman and Vernon (for a recent application, see e.g. Ref. [5] where semiclassical equations are derived for ϕ_1).

In matrix form,

$$
\mathbf{G}(x-x') = \begin{pmatrix} G^{++}(x-x') & G^{+-}(x-x') \\ G^{-+}(x-x') & G^{--}(x-x') \end{pmatrix},
$$

the propagator is now given by

$$
\mathbf{G}(x-x') \to R\mathbf{G}(x-x')R^T = \begin{pmatrix} iF(x-x') & G^{R}(x-x') \\ G^{A}(x-x') & 0 \end{pmatrix}, \tag{3.5}
$$

with

$$F(x-x') = \tfrac{1}{2}\langle \phi(x)\phi(x') + \phi(x')\phi(x)\rangle, \tag{3.6}$$

$$G^R(x-x') = G^A(x'-x) = i\theta(t-t')\langle [\phi(x),\phi(x')]\rangle. \tag{3.7}$$

The last equation can be used to define the spectral function[6]

$$\rho(x-x') = i\langle [\phi(x),\phi(x')]\rangle = G^R(x-x') - G^A(x-x'). \tag{3.8}$$

We will now use the KMS condition to relate the various introduced quantities. After Fourier transformation to momentum space, according to ($k = (k^0, \boldsymbol{k})$)

$$G^>(k) = \int d^4x\, e^{ik^0t - i\boldsymbol{k}\cdot\boldsymbol{x}}\, G^>(x),$$

the KMS condition (3.3) reads

$$G^>(k) = e^{\beta k^0}\, G^<(k).$$

From the KMS condition we find the following expressions in terms of the spectral function:

$$\begin{aligned} G^>(k) &= [n(k^0)+1]\rho(k), \qquad G^<(k) = n(k^0)\rho(k), \\ F(k) &= -i[n(k^0)+\tfrac{1}{2}]\rho(k), \\ n(k^0) &= \frac{1}{e^{\beta k^0}-1}. \end{aligned} \tag{3.9}$$

For $k^0 > 0$, $n(k^0)$ is the Bose distribution.

Notice that all components of the propagator are determined by the retarded propagator G^R. We could have used (3.9) to reduce the matrix propagator to a diagonal matrix $\mathrm{diag}(G^R, G^A)$, as is done in the so-called R/A formulation [17].[7] However, the formulation we use makes the comparison with the classical theory more direct, as we will show.

We end this section with some useful properties of the self-energy

$$\Sigma(k) = \mathbf{G}^{-1}(k) - \mathbf{G}_0^{-1}(k), \tag{3.10}$$

with $\mathbf{G}$ given by the 1,2-form (3.5) and the subscript 0 indicates the free propagator. The inverse propagator is given by

$$\mathbf{G}^{-1}(k) = \begin{pmatrix} 0 & G^A(k)^{-1} \\ G^R(k)^{-1} & [n(k^0)+\tfrac{1}{2}][G^R(k)^{-1} - G^A(k)^{-1}] \end{pmatrix},$$

where we used (3.9) and (3.8). It follows that Σ has the form

$$\Sigma(k) = \begin{pmatrix} \Sigma_{11}(k) & \Sigma_{12}(k) \\ \Sigma_{21}(k) & \Sigma_{22}(k) \end{pmatrix} = \begin{pmatrix} 0 & \Sigma_A(k) \\ \Sigma_R(k) & i\Sigma_F(k) \end{pmatrix},$$

with

[6] We have chosen the convention that $G^R(x), G^A(x), F(x)$ and $\rho(x)$ are all real.

[7] Note, however, that also in the R/A formulation the F propagator will appear; it is $\phi(k)$ in [17].

Fig. 2. Propagators: (a) $G_0^R(k) = G_0^A(-k)$, (b) $iF_0(k)$.

$$\Sigma_R(k) = \Sigma_A(-k) = \Sigma_A^*(k) = G^R(k)^{-1} - G_0^R(k)^{-1}, \tag{3.11}$$

$$\Sigma_F(k) = -i[n(k^0) + \tfrac{1}{2}][\Sigma_R(k) - \Sigma_A(k)] \tag{3.12}$$

From this we conclude that a calculation of the retarded self-energy $\Sigma_R(k)$ is sufficient to determine also the other components.

4. Perturbation theory in the quantum theory

Due to the fact that $\phi(x)$ and $\phi(x')$ do not commute in a quantum theory, different orderings of the fields along the contour give different n-point functions. In the classical theory, however, the typical two-point function to be calculated is

$$\langle \phi(x)\phi(x') \rangle_{\rm cl}, \tag{4.1}$$

with no special ordering (classically the fields commute of course). The quantum two-point function we are interested in is therefore

$$\tfrac{1}{2}\langle \phi(x)\phi(x') + \phi(x')\phi(x) \rangle = F(x-x') = \langle \phi_1(x)\phi_1(x') \rangle,$$

which reduces formally to (4.1) in the limit $\hbar \to 0$. We consider n-point connected Green functions where the external field is $\phi_1 = \frac{1}{2}(\phi_+ + \phi_-)$.

The free propagators are given by

$$G_0^R(k) = G_0^A(-k) = G_0^{A\,*}(k) = \frac{1}{\omega_k^2 - (k^0 + i\epsilon)^2}, \tag{4.2}$$

$$\begin{aligned} F_0(k) &= -i(n(k^0) + \tfrac{1}{2})\left(G_0^R(k) - G_0^A(k)\right) \\ &\overset{\epsilon \downarrow 0}{=} (n(k^0) + \tfrac{1}{2})\epsilon(k^0) 2\pi\delta(k_0^2 - \omega_k^2), \end{aligned} \tag{4.3}$$

with $\epsilon(k^0) = \theta(k^0) - \theta(-k^0)$. Note that the $i\epsilon$ dependence is unambiguously determined by the $i\epsilon$ dependence of the retarded (and advanced) Green functions. We keep ϵ finite throughout, to avoid products of delta functions.

The interaction part has to be expressed in terms of the ϕ_1, ϕ_2 fields using (3.4), which gives

$$-\int_{-\infty}^{\infty} dt \int d^3x \frac{\bar{\lambda}}{4!}\left(\phi_+^4 - \phi_-^4\right) = -\int_{-\infty}^{\infty} dt \int d^3x \frac{\bar{\lambda}}{4!}\left(4\phi_1^3\phi_2 + \phi_1\phi_2^3\right). \tag{4.4}$$

The Feynman rules are given in Figs. 2 and 3a, b. We represent the ϕ_1 field with a full line, and the ϕ_2 field with a dashed line. Hence the retarded and advanced Green functions, which interpolate between a ϕ_1 and a ϕ_2 field, are indicated with a dashed-full line.

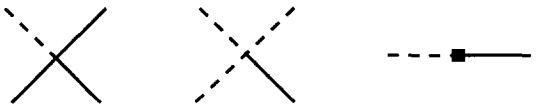

Fig. 3. Vertices, (a) $-\bar{\lambda}$, (b) $-\bar{\lambda}/4$, (c) $m_{\rm th}^2$.

The diagrams we are about to calculate contain the normal four-dimensional, zero-temperature divergences. As mentioned before, these will be treated using dimensional renormalization in the $\overline{\rm MS}$ scheme. The counterterms can be found in Appendix A.

As is well known, a consistent perturbative treatment needs a resummation of the so-called hard thermal loops (HTL's). In the scalar theory, the essential HTL is only the leaf diagram, which gives rise to the thermal mass $m_{\rm th}^2 = \bar{\lambda}T^2/24$. Resummation can be done by a simple addition and subtraction of the thermal mass [18–20]. The mass parameter that enters in the free propagator is now $m^2 = \bar{m}^2 + m_{\rm th}^2$, furthermore there is a new vertex, as shown in Fig. 3c. We will not try to improve perturbation theory any further, because our interest lies in the comparison with the classical theory, not in the improvement of perturbation theory.

We are now ready to calculate correlation functions in the quantum theory, but because we want to compare these with the ones obtained in the classical approximation, we first discuss the classical theory.

5. Classical correlation functions

In the following section we consider correlation functions in the classical theory. After the definition of classical correlation functions, we discuss the choice of parameters in the (effective) hamiltonian. Since the classical theory is supposed to be an approximation to the quantum theory at high temperature, the parameters in the classical hamiltonian are not arbitrary. We determine the parameters by restricting ourselves to equal time correlation functions, and then using the connection with the conventional dimensional reduction approach, as described in Section 2. We test whether this procedure makes sense for time-dependent correlation functions as well by a calculation of the classical two-point function up to two loops and the classical four-point function up to one loop and comparing these with the high-temperature expressions from the quantum theory.

We start by writing the hamiltonian, that corresponds to the classical action (3.2),

$$H = \int d^3x \left(\frac{1}{2}\pi^2 + \frac{1}{2}(\nabla\phi)^2 + \frac{1}{2}\nu^2\phi^2 + \frac{1}{4!}\lambda\phi^4 + \epsilon \right).$$

The classical two-point function is defined in the following way:

$$S(x-x') \equiv \langle \phi(x)\phi(x') \rangle_{\rm cl} \equiv \frac{\int \mathcal{D}\pi\mathcal{D}\phi\, e^{-\beta H(\pi,\phi)}\phi(x)\phi(x')}{\int \mathcal{D}\pi\mathcal{D}\phi\, e^{-\beta H(\pi,\phi)}}, \tag{5.1}$$

with $\phi(x)$ the solution of the equations of motion

$$\dot{\phi}(x) = \{\phi(x), H\},$$
$$\dot{\pi}(x) = \{\pi(x), H\}, \tag{5.2}$$

the curly brackets denoting the Poisson brackets. The initial conditions of these equations of motions are

$$\phi(\boldsymbol{x}, t_0) = \phi(\boldsymbol{x}), \qquad \pi(\boldsymbol{x}, t_0) = \pi(\boldsymbol{x}).$$

The integration in (5.1) is over the initial conditions, weighted with the Boltzmann weight.

As explained at the beginning of this section, the parameters in the hamiltonian are not arbitrary. We determine them by studying static correlation functions. If we restrict ourselves to $t = t'$, the fields are related by a canonical transformation with those at the initial time t_0. Then the integration over the canonical momenta is trivial, and we find the following expression:

$$S(\boldsymbol{x} - \boldsymbol{x}', 0) = \langle \phi(\boldsymbol{x}, t)\phi(\boldsymbol{x}', t)\rangle_{\rm cl} = \frac{\int \mathcal{D}\phi\, e^{-\beta V(\phi)}\phi(\boldsymbol{x})\phi(\boldsymbol{x}')}{\int \mathcal{D}\phi\, e^{-\beta V(\phi)}}, \tag{5.3}$$

which is just a correlation function in a three-dimensional field theory. In fact, the partition function is similar in form to the one obtained in the dimensional reduction approach (2.2). Using this observation we take the parameters in the effective hamiltonian to be given by the dimensional reduction matching relations, i.e. (2.6)–(2.11). The only thing that is not determined this way is a possible prefactor in front of the kinetic part of the hamiltonian, i.e. $\pi^2 \to z_\pi \pi^2$. We shall find that $z_\pi = 1$ to leading order in the matching of the classical and quantum theories.

Note that although we only match time-independent quantities, this will be sufficient to make the time-dependent quantities well defined and useful (in [7] we studied in particular the finiteness of the two-point function).

Now that we have determined the parameters in the hamiltonian, we can discuss the properties of time-dependent correlation functions. To make the comparison with the quantum theory straightforward, we introduce the classical counterparts of (3.7) and (3.8),

$$G^R_{\rm cl}(x - x') = G^A_{\rm cl}(x' - x) = -\theta(t - t')\langle\{\phi(x), \phi(x')\}\rangle_{\rm cl}, \tag{5.4}$$
$$\rho_{\rm cl}(x - x') = -\langle\{\phi(x), \phi(x')\}\rangle_{\rm cl} = G^R_{\rm cl}(x - x') - G^A_{\rm cl}(x - x'), \tag{5.5}$$

and the classical KMS condition (see Appendix B)

$$\frac{d}{dt}S(x - x') = -T\rho_{\rm cl}(x - x'). \tag{5.6}$$

If we specialize to the unperturbed problem ($\lambda = 0$), we can immediately solve the equations of motion and find

$$\phi_0(\boldsymbol{k}, t) = \int d^3x\, e^{-i\boldsymbol{k}\cdot\boldsymbol{x}}\phi_0(\boldsymbol{x}, t)$$

$$= \phi(\boldsymbol{k}) \cos \omega_k (t - t_0) + \frac{\pi(\boldsymbol{k})}{\omega_k} \sin \omega_k (t - t_0), \tag{5.7}$$

with $\omega_k^2 = \boldsymbol{k}^2 + m^2$, and where $\phi(\boldsymbol{k})$ and $\pi(\boldsymbol{k})$ are the Fourier components of the initial conditions. It is now easy to calculate the Poisson brackets in (5.4) to find

$$G_0^R(\boldsymbol{k}, t - t') = \theta(t - t') \frac{\sin \omega_k (t - t')}{\omega_k}. \tag{5.8}$$

Using the KMS condition (5.6) we find for the free two-point function (up to a constant)

$$S_0(\boldsymbol{k}, t - t') = T \frac{\cos \omega_k (t - t')}{\omega_k^2}, \tag{5.9}$$

which can also be found by explicitly performing the Gaussian integrations in (5.1). It is easy to make a connection with the quantum theory at this point. Fourier transforming the free retarded Green function in the quantum theory (4.2) back to time space gives (5.8). $G_0^R(x - x')$ is independent of T and $\hbar$. Hence we drop the subscript 'cl' for the free retarded and advanced Green functions. Fourier transforming the thermal propagator in the quantum theory, (4.3), gives

$$F_0(\boldsymbol{k}, t - t') = [n(\omega_k) + \tfrac{1}{2}] \frac{\cos \omega_k (t - t')}{\omega_k} = T \sum_n \frac{\cos \omega_k (t - t')}{\omega_n^2 + \omega_k^2}, \tag{5.10}$$

with the Matsubara frequencies $\omega_n = 2\pi n T$. We have used the identity

$$\frac{1}{\omega_k} [n(\omega_k) + \tfrac{1}{2}] = T \sum_{n=-\infty}^{\infty} \frac{1}{\omega_n^2 + \omega_k^2},$$

to obtain the last equality. Note that we have written the real-time correlation function as a sum over the Matsubara modes, familiar from the euclidean formulation. The $n = 0$ mode in (5.10) is precisely the classical propagator (5.9).

We conclude this section with a short discussion of $\hbar$. Up to now we have put $\hbar = c = 1$. However, $\hbar$ can always be restored by dimensional analysis, keeping $c = 1$. Since it has the dimension of energy times length ($[\hbar] = [El]$), we no longer have $[E] = [l^{-1}]$. By inspection of the classical hamiltonian, we find the following dimensions $[\phi^2] = [El^{-1}]$, $[m] = [l^{-1}]$, $[\lambda] = [E^{-1} l^{-1}]$; furthermore $[\boldsymbol{p}] = [p^0] = [l^{-1}]$ and for the self-energy $[\Sigma] = [l^{-2}]$. Using this we find that the thermal mass is proportional to $\hbar^{-1/2}$, $m_{\rm th}^2 = \bar{\lambda} T^2 / 24\hbar$. Thus we find that $\hbar$ is introduced in the classical theory through the matching relations.

In the following section we discuss the perturbation expansion in the classical theory.

6. Perturbation theory in the classical theory

To study classical time-dependent correlation functions in perturbation theory we can follow two approaches. The first approach is the one we followed in [7], the averaging

over the initial conditions is done at $t = t_0$, and t_0 is kept finite. Both the solution to the equations of motion and the Boltzmann weight are expanded in λ and correlation functions are calculated up to the desired order. As we have shown in [7] the final answer is independent of t_0, as expected in equilibrium.

We will now follow the thermal field theory approach, i.e. we use the classical KMS condition (5.6) to determine $S_0(k)$ to be

$$S_0(k) = S_0(\boldsymbol{k}, k^0) = -i\frac{T}{k^0}\left(G_0^R(k) - G_0^A(k)\right), \tag{6.1}$$

which is the analogue of (3.9). The Boltzmann weight $\exp(-\beta H)$ does not enter the perturbative calculations anymore and throughout we work in temporal momentum space. In Appendix C we illustrate both approaches with a simple example.

To calculate correlation functions in perturbation theory, we need to solve the equations of motion (5.2) perturbatively. In terms of the solution to the unperturbed problem $\phi_0(x)$ and the retarded Green function $G_0^R(x)$, the solution of the equations of motion to second order in the coupling constant given by

$$\begin{aligned}\phi(x) &= \phi_0(x) + \lambda\phi_1(x) + \lambda^2\phi_2(x)\\ &= \phi_0(x) - \lambda\int d^4x'\, G_0^R(x-x')\frac{1}{3!}\phi_0^3(x')\\ &\quad +\lambda^2\int d^4x'\, G_0^R(x-x')\frac{1}{2!}\phi_0^2(x')\int d^4x''\, G_0^R(x'-x'')\frac{1}{3!}\phi_0^3(x'').\end{aligned} \tag{6.2}$$

If we now want to calculate correlation functions like $\langle\phi(x_1)\phi(x_2)\rangle_{\rm cl}$ up to a certain order, we expand the $\phi(x)$'s as in (6.2), and order terms according to their power of λ. This gives rise to diagrams in the following way. The vertices are coming from the integrations over the retarded Green functions and the zero-order solutions, as in (6.2). The lines in the diagrams are either G_0^R lines, coming from the solution (6.2), or S_0 lines, coming from the contractions of products of ϕ_0. In diagrams we use the same representation as in the quantum case, i.e. the dashed-full lines represent the retarded and advanced Green functions, and the full line the thermal propagator S_0.

A straightforward calculation of correlation functions, as defined in (5.1), results in the connected diagrams. As can be deduced from the expressions in [7], the two-point function can be written in the form

$$S = S_0 - S_0\Sigma_{A,\rm cl}G^A - G_0^R\Sigma_{R,\rm cl}S - G_0^R\Sigma_{F,\rm cl}G^A,$$

which is just the analogue of the F component of $\mathbf{G} = \mathbf{G}_0 - \mathbf{G}_0\Sigma\mathbf{G}$ obtained by multiplication of (3.10) with $\mathbf{G}_0$ and $\mathbf{G}$ from the left and right. In the following we will truncate the external lines and concern ourselves only with the 1PI diagrams. We use the same (1,2) notation as in the quantum case to denote the different types of diagrams, e.g. the classical retarded self-energy is written as $\Sigma_{R,\rm cl}(p) = \Sigma_{21,\rm cl}(p)$.

A last remark is related to the resummation in the quantum theory. In the classical perturbation expansion, the thermal mass which is generated through the matching

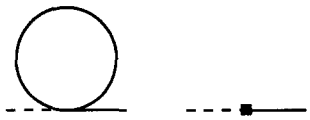

Fig. 4. Retarded self-energy $\Sigma_R^{(1)}$; the second diagram, coming from resummation, is only present in the quantum theory.

prescription (2.7), is included in the zero-order mass parameter, just as in the quantum theory after resummation.

We are now ready to compute time-dependent correlation functions and compare the classical result with the full quantum field theory result. We will study the self-energy and the four-point function in the following sections.

7. The self-energy

In this section we calculate the self-energy to two loops in both the quantum and the classical theory. To simplify the notation in the quantum theory and avoid writing $\int d^{4-2\epsilon}k$, etc., we shall assume the counterterms of the $\overline{\text{MS}}$ scheme to be absorbed into the symbol $\int d^4k$.

7.0.1. First-order self-energy

For the one-loop retarded self-energy in the quantum theory, we get

$$\Sigma_R^{(1)} = \tfrac{1}{2}\bar{\lambda}\int \frac{d^4k}{(2\pi)^4} F_0(k) - m_{\text{th}}^2. \tag{7.1}$$

The diagrams are shown in Fig. 4. Performing the integral leads to

$$\Sigma_R^{(1)} = -\bar{\lambda}\frac{mT}{8\pi} - \bar{\lambda}\frac{m^2}{32\pi^2}\log\frac{\bar{\mu}^2}{\mu_T^2} + \mathcal{O}(T^{-2}).$$

Furthermore we find from (3.11) $\Sigma_A^{(1)} = \Sigma_R^{(1)}$ and hence from (3.12) $\Sigma_F^{(1)} = 0$. This result can also be found by a calculation of the relevant Feynman diagram, which is

$$\Sigma_F^{(1)} = -\frac{1}{4}\bar{\lambda}\int \frac{d^4k}{(2\pi)^4} G_0^R(k) = 0,$$

because all the poles are on the same side of the real k^0 axis in the complex k^0 plane (see e.g. also Ref. [17]). The result is that the second vertex in (4.4) does not contribute to this order.

The classical retarded self-energy to one loop is given by

$$\Sigma_{R,\text{cl}}^{(1)} = \tfrac{1}{2}\lambda\int \frac{d^4k}{(2\pi)^4} S_0(k) - \lambda m_1^2, \tag{7.2}$$

where m_1^2 is given by (2.8). Comparing the classical and the quantum results, we see that the classical result can simply be obtained with the substitution $F_0 \to S_0$. Notice

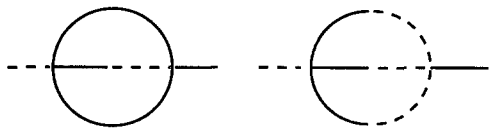

Fig. 5. Setting sun contribution to the retarded self-energy $\Sigma_R^{\rm sun}$; in the quantum case both diagrams contribute, in the classical case only the first one is present.

that to first order $\bar{\lambda}$ and λ are equal, as can be seen in the matching relation (2.10). The difference appears in higher order. The final answer is

$$\Sigma^{(1)}_{R,\rm cl} = -\lambda\frac{mT}{8\pi} - \lambda\frac{m^2}{32\pi^2}\log\frac{\bar{\mu}^2}{\mu_T^2}.$$

The leading $\mathcal{O}(T)$ term (after resummation in the quantum theory) is correctly reproduced by the classical one-loop expression. Indeed, as can be seen by explicitly writing $\hbar$, the term proportional to T is classical. The term with the logarithm, coming from the matching condition (2.8), is proportional to $\hbar$. We end the discussion of the one-loop self-energy with the remark that since this one-loop diagram is momentum independent, the fact that we are studying the *time-dependent* two-point function does not come into play, and the outcome is the standard dimensional reduction result.

We now turn to the second-order contributions.

7.0.2. Second-order retarded self-energy: the setting sun diagrams

The second-order contribution to the self-energy is more interesting, because of explicit momentum dependence of the setting sun diagrams.

In the quantum theory the retarded setting sun diagrams are given by[8]

$$\Sigma_R^{\rm sun}(p) = -\frac{1}{2}\bar{\lambda}^2\int\frac{d^4k_1}{(2\pi)^4}\frac{d^4k_2}{(2\pi)^4}\Big[F_0(k_1)F_0(k_2)G_0^R(p-k_1-k_2) \tag{7.3}$$

$$-\frac{1}{12}G_0^R(k_1)G_0^R(k_2)G_0^R(p-k_1-k_2)\Big]. \tag{7.4}$$

The diagrams are given in Fig. 5. Note there is no explicit temperature dependence in the second diagram.

After performing the temporal momentum integrals the first diagram can be expressed as

$$\Sigma^{\rm sun}_{R,\rm a}(p) = -\frac{1}{2}\bar{\lambda}^2\sum_{\{\epsilon_i\}}\int d\Phi_{123}(p)\,(n_{k_1}+\tfrac{1}{2})(n_{k_2}+\tfrac{1}{2})\frac{\epsilon_3}{p^0+i\epsilon+\epsilon_i\omega_{k_i}}, \tag{7.5}$$

[8] Diagrams that contain a subdiagram such as

$$\int\frac{d^4k}{(2\pi)^4}G_0^R(k)G_0^R(p+k),$$

are not explicitly written, because they are zero (all the poles are on the same side of the real k^0 axis in the complex k^0 plane).

where $d\Phi_{123}(\boldsymbol{p})$ was introduced in (2.5), $n_k = n(\omega_k)$ and

$$\epsilon_i \omega_{k_i} = \epsilon_1 \omega_{k_1} + \epsilon_2 \omega_{k_2} + \epsilon_3 \omega_{k_3}.$$

The sum is over $\epsilon_i = \pm 1$, with $i = 1,2,3$. The expression can be written in a symmetric way by a permutation of the (1,2,3) indices.

The second diagram can be expressed as

$$\Sigma^{\rm sun}_{R,\rm b}(p) = -\frac{\bar{\lambda}^2}{24} \sum_{\{\epsilon_i\}} \int d\Phi_{123}(\boldsymbol{p}) \, \frac{\epsilon_1\epsilon_2\epsilon_3}{p^0 + i\epsilon + \epsilon_i \omega_{k_i}}. \tag{7.6}$$

One might be surprised that we find two diagrams that contribute to the retarded setting sun self-energy. However, it is easy to check that the sum of (7.5) and (7.6) gives precisely the expression that is obtained in the imaginary-time formalism after an analytic continuation to real external frequencies [20].

The real part of the self-energy contains the standard $T = 0$ divergence, and a momentum independent subdivergence [18,19]. It satisfies $\mathrm{Re}\,\Sigma^{\rm sun}_R(\boldsymbol{p}, -p^0) = \mathrm{Re}\,\Sigma^{\rm sun}_R(\boldsymbol{p}, p^0)$. The imaginary part obeys $\mathrm{Im}\,\Sigma^{\rm sun}_R(\boldsymbol{p}, p^0) = -\mathrm{Im}\,\Sigma^{\rm sun}_R(\boldsymbol{p}, -p^0)$, so that we can restrict ourselves to $p^0 > 0$. It can be written as [20]

$$-\mathrm{Im}\,\Sigma^{\rm sun}_R(p) = g_1(p) + g_2(p),$$

with

$$g_1(p) = \frac{\bar{\lambda}^2}{12}(e^{p^0/T} - 1) \int d\Phi_{123}(\boldsymbol{p})\, 2\pi\delta(p^0 - \omega_{k_1} - \omega_{k_2} - \omega_{k_3}) n_{k_1} n_{k_2} n_{k_3},$$

$$g_2(p) = \frac{\bar{\lambda}^2}{4}(e^{p^0/T} - 1) \int d\Phi_{123}(\boldsymbol{p})\, 2\pi\delta(p^0 + \omega_{k_1} - \omega_{k_2} - \omega_{k_3})(1 + n_{k_1}) n_{k_2} n_{k_3},$$

representing three-body decay and Landau damping respectively. The on-shell plasmon damping rate

$$\gamma = \frac{-\mathrm{Im}\,\Sigma^{\rm sun}_R(\boldsymbol{0}, m)}{2m} = \frac{g_2(\boldsymbol{0}, m)}{2m} = \frac{\bar{\lambda}^{3/2} T}{128\sqrt{6}\pi} \left(1 + \mathcal{O}(\sqrt{\bar{\lambda}} \log \bar{\lambda})\right), \tag{7.7}$$

as calculated in [19,20]. The last equality is valid in the case that the thermal mass is much larger than the $\overline{\rm MS}$ mass.

In the classical theory we find the following expression:

$$\Sigma^{\rm sun}_{R,\rm cl}(p) = -\tfrac{1}{2}\lambda^2 \int \frac{d^4k_1}{(2\pi)^4} \frac{d^4k_2}{(2\pi)^4} S_0(k_1) S_0(k_2) G^R_0(p - k_1 - k_2) - \lambda^2 m_2^2, \tag{7.8}$$

with m_2^2 given by (2.9). It is similar to the quantum expression (7.3) after the replacement $S_0 \to F_0$ ($\bar{\lambda}$ and λ are the same to this order). After this replacement we see that, concerning the explicit temperature dependence, (7.3) is $\mathcal{O}(T^2)$ and (7.4) is $\mathcal{O}(T^0)$. Indeed, in the classical theory, which is supposed to be valid only to leading order in T, there is no analogue of (7.4). Performing the temporal momentum integrals, we get

$$\Sigma^{\rm sun}_{R,{\rm cl}}(p) = -\tfrac{1}{2}\lambda^2 T^2 \sum_{\{\epsilon_i\}} \int d\Phi_{123}(\boldsymbol{p})\, \frac{1}{\omega_{k_1}\omega_{k_2}\omega_{k_3}}\, \frac{\epsilon_3\omega_{k_3}}{p^0 + i\epsilon + \epsilon_i\omega_{k_i}} - \lambda^2 m_2^2$$
$$= -\frac{\lambda^2 T^2}{6} \int d\Phi_{123}(\boldsymbol{p})\, \frac{8}{\omega_{k_1}\omega_{k_2}\omega_{k_3}} + \frac{p^0}{T} \int \frac{d\Omega}{2\pi}\, \frac{w(\boldsymbol{p},\Omega)}{p^0 + i\epsilon + \Omega} - \lambda^2 m_2^2, \tag{7.9}$$

with

$$w(\boldsymbol{p},\Omega) = \frac{\lambda^2}{6} \sum_{\{\epsilon_i\}} \int d\Phi_{123}(\boldsymbol{p})\, 2\pi\delta(\Omega - \epsilon_i\omega_{k_i})\, \frac{T^3}{\omega_{k_1}\omega_{k_2}\omega_{k_3}}\,.$$

In obtaining this result we symmetrized $\epsilon_3\omega_{k_3} \to \epsilon_i\omega_{k_i}/3$. Notice that the first term in (7.9) is real, independent of p^0 and logarithmically divergent. This divergence is cancelled with the counterterm m_2^2, cf. (2.3) and (2.9). The weight function $w(\boldsymbol{p},\Omega)$ is finite and behaves like Ω^{-1} as $\Omega \to \infty$. Hence, the second term given by the dispersion relation in (7.9) is finite. So we arrive at the conclusion already obtained in [7], namely the classical theory can be made finite with just the counterterms of the static theory. Furthermore, as we show in Appendix D, the difference between the quantum and classical expressions for the two-loop self-energy is subleading for $T \to \infty$ and $\bar{\lambda} \to 0$.

It is interesting to compare the imaginary parts of the self-energies. Similar to the quantum case we can write the imaginary part of the classical self-energy as ($p^0 > 0$)

$$-{\rm Im}\,\Sigma^{\rm sun}_{R,{\rm cl}}(p) = g_{1,{\rm cl}}(p) + g_{2,{\rm cl}}(p),$$

with

$$g_{1,{\rm cl}}(p) = \frac{\lambda^2 p^0}{12T} \int d\Phi_{123}(\boldsymbol{p})\, 2\pi\delta(p^0 - \omega_{k_1} - \omega_{k_2} - \omega_{k_3})\, \frac{T^3}{\omega_{k_1}\omega_{k_2}\omega_{k_3}}\,,$$
$$g_{2,{\rm cl}}(p) = \frac{\lambda^2 p^0}{4T} \int d\Phi_{123}(\boldsymbol{p})\, 2\pi\delta(p^0 + \omega_{k_1} - \omega_{k_2} - \omega_{k_3})\, \frac{T^3}{\omega_{k_1}\omega_{k_2}\omega_{k_3}}\,.$$

Comparing the prefactors in these expressions with the quantum counterparts, we see explicitly that we must restrict ourselves to external frequencies $|p^0| \ll T$ in order for the classical approximation to be valid. The classical on-shell damping rate is given by

$$\gamma_{\rm cl} = -\frac{{\rm Im}\,\Sigma^{\rm sun}_{R,{\rm cl}}(\boldsymbol{0},m)}{2m} = \frac{g_{2,{\rm cl}}(\boldsymbol{0},m)}{2m} = \frac{\lambda^2 T^2}{1536\pi m} \approx \frac{\lambda^{3/2} T}{128\sqrt{6\pi}},$$

where we used the matching relation (2.7) to obtain the last expression. After matching it indeed equals the quantum damping rate (7.7), as we have shown earlier in [7].

Introducing $\hbar$ leads to the observation that the damping rate is independent of $\hbar$, if the classical mass parameter is arbitrary. However, taking the classical mass parameter according to the matching relation (2.7), gives a damping rate which is proportional to $\hbar^{1/2}$ (when the thermal mass is much larger than the $\overline{\rm MS}$ mass). This $\hbar$ dependence arises solely from the $\hbar$ dependence of the thermal mass.

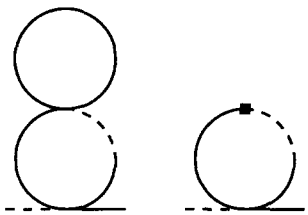

Fig. 6. Tadpole contributions to the retarded self-energy $\Sigma_R^{(2)\mathrm{tp}}$; the one-loop diagram, with the vertex due to resumming, is only present in the quantum case.

Finally, the comparison between the quantum and the classical expressions in Appendix D, shows that the p^0 dependence is the same in leading order. Therefore we conclude that the possible prefactor z_π in the kinetic part $\int d^3x\, z_\pi \pi^2/2$ of the hamiltonian, is equal to one to this order.

7.0.3. Second-order retarded self-energy: the tadpole diagrams

The tadpole diagrams are less interesting than the setting sun diagrams. Because they are momentum independent, the fact that we are concerned with time-dependent correlation functions does not play a role. The matching procedure is identical to dimensional reduction for static quantities. Therefore we will just give the expressions for completeness.

In the quantum theory we find the two loop and the one loop (with the vertex due to resumming) expressions

$$\Sigma_R^{(2)\mathrm{tp}} = -\frac{1}{2}\bar{\lambda}^2 \int \frac{d^4k}{(2\pi)^4} F_0(k) G_0^R(k) \int \frac{d^4k'}{(2\pi)^4} F_0(k') + \bar{\lambda} m_{\mathrm{th}}^2 \int \frac{d^4k}{(2\pi)^4} F_0(k) G_0^R(k),$$

which are shown in Fig. 6. We have not shown the diagrams with $\overline{\mathrm{MS}}$ counterterms insertions [18,19]. Of course the tadpole contribution is real.

In the classical theory, we find the following second-order contribution:

$$\Sigma_{R,\mathrm{cl}}^{(2)\mathrm{tp}} = -\frac{1}{2}\lambda^2 \int \frac{d^4k}{(2\pi)^4} S_0(k) G_0^R(k) \int \frac{d^4k'}{(2\pi)^4} S_0(k') + \lambda^2 m_1^2 \int \frac{d^4k}{(2\pi)^4} S_0(k) G_0^R(k).$$

Again the correspondence with the quantum expression follows from $F_0 \to S_0$.

7.0.4. Second-order F component of the self-energy

For completeness we also give the F component of the self-energy. A detailed calculation is not necessary because it is related to the retarded self-energy through the KMS condition (3.12). It is however again instructive to compare the quantum with the classical expressions.

In the quantum theory we find

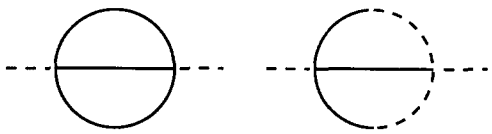

Fig. 7. Setting sun contribution to the F component of the self-energy $\Sigma_F^{(2)}$; in the classical case the second diagram is absent.

$$\Sigma_F^{(2)}(p) = -\bar{\lambda}^2 \int \frac{d^4k_1}{(2\pi)^4}\frac{d^4k_2}{(2\pi)^4}\Big[\frac{1}{6}F_0(k_1)F_0(k_2)F_0(p-k_1-k_2) \tag{7.10}$$

$$-\frac{1}{8}G_0^R(k_1)G_0^R(k_2)\,(F_0(k_1+k_2-p)+F_0(k_1+k_2+p))\Big], \tag{7.11}$$

shown in Fig. 7. As can be seen in Appendix A, there is no counterterm for these diagrams, they are finite by themselves.

In the classical theory we get

$$\Sigma_{F,\mathrm{cl}}^{(2)}(p) = -\frac{\lambda^2}{6}\int \frac{d^4k_1}{(2\pi)^4}\frac{d^4k_2}{(2\pi)^4}S_0(k_1)S_0(k_2)S_0(p-k_1-k_2).$$

Again we see that the classical expression is similar to the quantum expression (7.10) after the replacement $F_0 \to S_0$. The second diagram (7.11) has no classical counterpart, analogous to the situation for the retarded setting sun diagrams (7.3) and (7.4).

In the following section we take a look at the four-point function.

8. The four-point function

In this section we give the results for the four-point vertex function. Since the static theory is super-renormalizable, the self-coupling in the effective theory only receives a finite contribution due to matching (2.10). We show that also the time-dependent four-point function is finite. Furthermore we show that the classical result gives the leading order quantum result.

The connected time-dependent classical four-point function is defined by

$$G_{\mathrm{cl}}(x_1,x_2,x_3,x_4) = \langle\phi(x_1)\phi(x_2)\phi(x_3)\phi(x_4)\rangle_{\mathrm{cl}}$$
$$-\langle\phi(x_1)\phi(x_2)\rangle_{\mathrm{cl}}\langle\phi(x_3)\phi(x_4)\rangle_{\mathrm{cl}} + \text{perm.}$$

We extract the 1PI part in the usual way by an amputation of the external lines and use the obvious 1, 2 notation to indicate the full and dashed external lines. The external momenta are written as $p \equiv p_1 + p_2 = p_3 + p_4$. Diagrams that can simply be obtained by a permutation of the external lines are not explicitly written. We also give the results for the zero-loop vertex function, because this contains already non trivial information.

We start with the 1112 vertex function in the quantum theory. To second order in the coupling constant we find

$$\Gamma_{1112}^{(0+1)}(p) = -\frac{\bar{\lambda}}{3} + \bar{\lambda}^2\int\frac{d^4k}{(2\pi)^4}G_0^R(k+p)F_0(k) \tag{8.1}$$

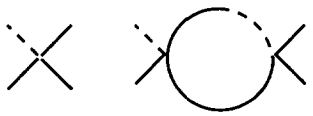

Fig. 8. Zero- and one-loop contribution to the vertex function Γ_{1112}.

shown in Fig. 8. The integral expression reads

$$\Gamma^{(1)}_{1112}(p) = \bar{\lambda}^2 \int \frac{d^3k}{(2\pi)^3} \frac{1}{8\omega_k\omega_{k+p}} \times \left[(n_k + n_{k+p} + 1) \left(\frac{1}{p^0 + \omega_k + \omega_{k+p}} - \frac{1}{p^0 - \omega_k - \omega_{k+p}} \right) + (n_{k+p} - n_k) \left(\frac{1}{p^0 + \omega_k - \omega_{k+p}} - \frac{1}{p^0 - \omega_k + \omega_{k+p}} \right) \right], \tag{8.2}$$

with $p^0 = p^0 + i\epsilon$. This quantum result contains the usual logarithmic $T = 0$ divergence which is cancelled with the counterterm (see Appendix A). The leading order behaviour in the temperature is $\mathcal{O}(T)$.

In the classical case we find the, by now expected, result

$$\Gamma^{(0+1)}_{1112,\mathrm{cl}}(p) = -\frac{\lambda}{3} + \lambda^2 \int \frac{d^4k}{(2\pi)^4} G^R_0(k+p) S_0(k) \tag{8.3}$$

The integral expression is given by (8.2) after the replacement $n_k + \frac{1}{2} \to T/\omega_k$. It is finite and it gives the leading $\mathcal{O}(T)$ quantum result. We discuss the difference between the quantum and the classical expressions in detail in Appendix D.

For the case where the external spatial momenta $\boldsymbol{p}$ are zero, we have calculated the one-loop contribution explicitly using standard high-temperature techniques with the result ($y = m/T, s = p^0/2T$)

$$\bar{\lambda}^{-2}\Gamma^{(1)}_{1112}(\mathbf{0}, p^0) = \frac{1}{16\pi} \frac{1}{\sqrt{y^2 - s^2} + y} + \frac{1}{8\pi} \sum_{l=1}^{\infty} \frac{\sqrt{y^2 + (2\pi l)^2} - \sqrt{y^2 - s^2} - 2\pi l}{(2\pi l)^2 + s^2} + \frac{1}{16\pi^2} \sum_{n=1}^{\infty} (-1)^n \left(\frac{s}{2\pi} \right)^{2n} \zeta(2n+1) + \frac{1}{32\pi^2} \left(2 + \log \frac{\bar{\mu}^2}{\mu_T^2} \right),$$

with $\zeta(n)$ the Riemann zeta function. The classical result is simply

$$\bar{\lambda}^{-2}\Gamma^{(1)}_{1112,\mathrm{cl}}(\mathbf{0}, p^0) = \frac{1}{16\pi} \frac{1}{\sqrt{y^2 - s^2} + y} + \frac{1}{32\pi^2} \log \frac{\bar{\mu}^2}{\mu_T^2},$$

which is indeed the leading order quantum result when $m, p^0 \ll T$. In obtaining this formula, we used the matching formula (2.10) to write λ in terms of $\bar{\lambda}$.

In the quantum theory we also have a 1222 vertex function. It turns out to be

$$\Gamma^{(0+1)}_{1222}(p) = \tfrac{1}{4}\Gamma^{(0+1)}_{1112}(p), \tag{8.4}$$

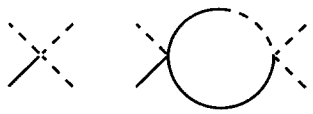

Fig. 9. Zero- and one-loop contribution to the vertex function Γ_{1222} in the quantum theory; in the classical theory it is zero.

Fig. 10. One-loop contribution to the vertex function Γ_{1212}; in the classical case only the first diagram is present.

and hence differs only in the external lines from Γ_{1112}, as shown in Fig. 9. Adding the external lines to the 1PI diagram to obtain the connected four-point function, and using the fact that the external momenta p, p^0 and the mass m are small with respect to the temperature T, we find that the contribution from Γ_{1222} to the connected four-point function is $\mathcal{O}(T^{-2})$ suppressed with respect to the contribution from the Γ_{1112} vertex function. Indeed, in the classical theory we do not have a 1222-type of vertex function.

For completeness we also give the result for the 1212 vertex function. It is related to the 1112 vertex function, as explained in Appendix E. In the quantum theory we find

$$\Gamma^{(1)}_{1212}(p) = \frac{\bar{\lambda}^2}{2}\int \frac{d^4k}{(2\pi)^4}\left(F_0(k)F_0(k+p) - \tfrac{1}{4}\left(G_0^R(k+p) + G_0^R(k-p)\right)G_0^A(k)\right), \tag{8.5}$$

there is no counterterm. The second diagram contains no explicit temperature dependence. In the classical theory we have

$$\Gamma^{(1)}_{1212,\mathrm{cl}}(p) = \frac{\bar{\lambda}^2}{2}\int \frac{d^4k}{(2\pi)^4} S_0(k)S_0(k+p). \tag{8.6}$$

The diagrams are shown in Fig. 10. Again the identification is straightforward, after the replacement $F_0 \to S_0$, the second quantum diagram is $\mathcal{O}(T^{-2})$ suppressed, and there is only one classical contribution.

This completes the discussion of the four-point function. We conclude that the leading order quantum results are classical, when $p, p^0, m \ll T$.

9. Conclusion

In this paper we looked at real-time correlation functions in $\lambda\phi^4$ theory. We made a diagrammatic comparison between real-time correlation functions in quantum field theory and in the classical theory. The conclusions are twofold.

The first conclusion is the one already obtained in [7], namely the classical theory is renormalizable. A set of local counterterms is sufficient to cancel the divergences

that arise in the perturbative calculations. These counterterms are exactly the counterterms needed for the static correlation functions, which are dictated by the superrenormalizability of the static theory. This observation is useful for a non-perturbative calculation of time-dependent classical correlation functions, e.g. numerically on a lattice. Lattice artefacts in physical observables can be rendered negligible, in principle, by tuning of bare parameters.

The second conclusion is that at high temperature and small coupling the classical theory can approximate the quantum theory. For this it is necessary to make a suitable choice of parameters in the effective classical hamiltonian, for which we used standard dimensional reduction matching relations for time-independent correlation functions. High temperature here means $\overline{\rm MS}$ mass parameter $\bar{m}$, external momenta $\boldsymbol{p}$ and frequencies p^0 much smaller than T, and $\overline{\rm MS}$ scale $\bar{\mu}$ near $\mu_T \approx 7T$. More precisely we found the condition $\bar{m}, \boldsymbol{p}, |p^0| \leq \mathcal{O}(\sqrt{\bar{\lambda}}T)$, and $\bar{\lambda} \ll 1$.

An extension of these methods to gauge theories meets the problem that the perturbative infinities of the hot classical theory are similar in form to the hard thermal loop action [21,22], hence non-local (and on a lattice even non-rotational invariant) [4,23]. Yet, it may still be advantageous to view these non-local infinities as to be cancelled by corresponding non-local counterterms, such that in principle the regularization can be removed. The ambiguity in the finite parts left after cancellation of the divergencies can then be removed by matching with the standard hard thermal loop action. Such a procedure may be able to avoid the problem of regularization dependence, which enters approaches in which the cutoff is kept finite, of order of the temperature [4,24]. Partial matching has already been used in numerical simulations of the classical SU(2)-Higgs theory at finite temperature, in which the effective parameters of the Higgs field were determined via dimensional reduction [25–27]. The hard thermal loop effects of the gauge field were not matched, however.

Acknowledgements

This work is supported by FOM.

Appendix A. Counterterms for the quantum theory

We assume the quantum theory to be dimensionally renormalized in $d = 4 - 2\epsilon$ dimensions according to the $\overline{\rm MS}$ scheme. The relation between μ of the MS scheme and $\bar{\mu}$ of the $\overline{\rm MS}$ scheme is

$$\mu = \bar{\mu}(4\pi e^{-\gamma})^{-1/2}.$$

The counterterms ct in the actions (2.1, 3.2) are given by the coefficients A – C below, taken from Ref. [18],

$$\mathrm{ct} = \frac{1}{2} A \left((\partial_\mu \phi_+)^2 - (\partial_\mu \phi_-)^2 \right) + \frac{1}{2} B \bar{m}^2 \left(\phi_+^2 - \phi_-^2 \right) + \frac{1}{4!} C \bar{\mu}^{2\epsilon} \bar{\lambda} \left(\phi_+^4 - \phi_-^4 \right)$$
$$= A \partial_\mu \phi_1 \partial^\mu \phi_2 + B \bar{m}^2 \phi_1 \phi_2 + \frac{\bar{\lambda}}{4!} C \bar{\mu}^{2\epsilon} \left(4 \phi_1 \phi_2^3 + \phi_1^3 \phi_2 \right).$$

The actual values of the counterterms are, up to the desired order and in the MS scheme

$$A = \bar{\lambda}^2 A_2 = -\hat{\lambda}^2 / 24\epsilon, \qquad \hat{\lambda} = \bar{\lambda} / 16\pi^2,$$
$$B = \bar{\lambda} B_1 + \bar{\lambda}^2 B_2 = \hat{\lambda}/2\epsilon + \hat{\lambda}^2 (1/2\epsilon^2 - 1/4\epsilon),$$
$$C = \bar{\lambda} C_1 = 3\hat{\lambda}/2\epsilon.$$

Appendix B. The classical KMS condition

The classical KMS condition can be derived in the following way (see e.g. Ref. [28]).

Consider classical observables A and B, obeying the equations of motion $\dot{A} = \{A, H\}$, $\dot{B} = \{B, H\}$, and look at the following correlation function:

$$\langle A(x) B(x') \rangle_{\mathrm{cl}} = \frac{1}{Z} \int \mathcal{D}\pi \mathcal{D}\phi \, e^{-\beta H(\pi, \phi)} A(x) B(x').$$

Taking the derivative with respect to t and using the equations of motion and the fact that the equations of motion and the canonical average are governed by the same hamiltonian, easily leads to

$$\frac{d}{dt} \langle A(x) B(x') \rangle_{\mathrm{cl}} = \langle \{A(x), H\} B(x') \rangle_{\mathrm{cl}} = \frac{1}{\beta} \langle \{A(x), B(x')\} \rangle_{\mathrm{cl}}.$$

Taking for both A and B ϕ and using the definition for the classical spectral function

$$\rho_{\mathrm{cl}}(x - x') = -\langle \{\phi(x), \phi(x')\} \rangle_{\mathrm{cl}}$$

gives the classical KMS condition

$$\beta \frac{d}{dt} S(x - x') = -\rho_{\mathrm{cl}}(x - x'),$$

or, in temporal momentum space,

$$S(k) = -\frac{T}{k^0} i \rho_{\mathrm{cl}}(k).$$

Appendix C. The classical 'mass derivative formula'

In thermal field theory the doubling of the fields, the vertical part of the contour, the $i\epsilon$ regularization and the KMS condition, are all closely related. This can be checked in explicit calculations, i.e. with the so-called mass derivative formula [14,15]. We will repeat this calculation for the classical theory.

Consider the following hamiltonian:

$$H = \int d^3x \left(\tfrac{1}{2}\pi^2 + \tfrac{1}{2}(\nabla\phi)^2 + \tfrac{1}{2}m^2\phi^2 + \tfrac{1}{2}\kappa\phi^2\right) = H_0 + \int d^3x \tfrac{1}{2}\kappa\phi^2.$$

The two-point function, as defined in (5.1), is exactly given by

$$S(\boldsymbol{k}, t_1 - t_2) = T\frac{\cos[\sqrt{\omega_k^2 + \kappa}(t_1 - t_2)]}{\omega_k^2 + \kappa},$$

with $\omega_k^2 = \boldsymbol{k}^2 + m^2$. We will, however, interpret the κ term as an interaction vertex and calculate the first-order correction in κ to the two-point function. To check the result we can compare it with the exact result after expansion

$$\begin{aligned} S(\boldsymbol{k}, t_1 - t_2) &= S_0(\boldsymbol{k}, t_1 - t_2) + \kappa S_1(\boldsymbol{k}, t_1 - t_2) + \mathcal{O}(\kappa^2), \\ S_1(\boldsymbol{k}, t_1 - t_2) &= -\frac{T}{2\omega_k^4}\left(\omega_k(t_1 - t_2)\sin\omega_k(t_1 - t_2) + 2\cos\omega_k(t_1 - t_2)\right). \end{aligned} \quad \text{(C.1)}$$

We now obtain this result by solving the equations of motion perturbatively as

$$\phi(\boldsymbol{k}, t) = \phi_0(\boldsymbol{k}, t) + \kappa\phi_1(\boldsymbol{k}, t) + \mathcal{O}(\kappa^2),$$

with the initial conditions

$$\phi_0(\boldsymbol{k}, t_0) = \phi(\boldsymbol{k}), \qquad \dot{\phi}_0(\boldsymbol{k}, t_0) = \pi(\boldsymbol{k}), \qquad \phi_1(\boldsymbol{k}, t_0) = \dot{\phi}_1(\boldsymbol{k}, t_0) = 0.$$

$\phi_0(\boldsymbol{k}, t)$ is given by (5.7), and

$$\phi_1(\boldsymbol{k}, t) = \int_{t_0}^{\infty} dt'\, G_0^R(\boldsymbol{k}, t - t')\phi_0(\boldsymbol{k}, t').$$

We will now calculate the first-order correction in two ways.

(1) Keeping t_0 finite.

We keep t_0 finite and expand also the Boltzmann weight as

$$e^{-\beta H} = e^{-\beta H_0}\left(1 - \beta\int d^3x \tfrac{1}{2}\kappa\phi_0^2(\boldsymbol{x}, t_0)\right).$$

$S_1(\boldsymbol{k}, t_1 - t_2)$ is found by collecting the two contributions proportional to κ. The result is

$$S_1(\boldsymbol{k}, t_1 - t_2) = -\beta S_0(\boldsymbol{k}, t_1 - t_0)S_0(\boldsymbol{k}, t_0 - t_2) \quad \text{(C.2)}$$

$$+ \int_{t_0}^{\infty} dt'\, G_0^R(\boldsymbol{k}, t_1 - t')S_0(\boldsymbol{k}, t' - t_2) + (t_1 \leftrightarrow t_2). \quad \text{(C.3)}$$

(C.2) is coming from the first-order expansion of the Boltzmann weight (proportional to β) and (C.3) from the first-order solution to the equations of motion. Performing the integral gives

$$S_1(\boldsymbol{k}, t_1 - t_2) = -\frac{T}{\omega_k^4} \cos\omega_k(t_1 - t_0) \cos\omega_k(t_0 - t_2)$$
$$-\frac{T}{\omega_k^3} \int_{t_0}^{t_1} dt' \sin\omega_k(t_1 - t') \cos\omega_k(t' - t_2) + (t_1 \leftrightarrow t_2)$$
$$= -\frac{T}{2\omega_k^4} \left(\omega_k(t_1 - t_2) \sin\omega_k(t_1 - t_2) + 2\cos\omega_k(t_1 - t_2)\right).$$

As expected, the t_0 dependence has dropped out. We stress that taking into account the terms coming from the Boltzmann weight is crucial for this. We recover the result (C.1).

(2) Thermal field theory approach.

In the standard thermal field theory approach t_0 is sent to $-\infty$ and contributions from the Boltzmann weight (i.e. (C.2)) are omitted. The part coming from the equations of motion (i.e. (C.3)) is written in temporal momentum space. We get

$$S_1(k) = \left(G_0^R(k) + G_0^A(k)\right) S_0(k),$$

with S_0 determined by the KMS condition

$$S_0(k) = -i\frac{T}{k^0}\left(G_0^R(k) - G_0^A(k)\right). \tag{C.4}$$

This leads to

$$S_1(\boldsymbol{k}, t_1 - t_2) = \int \frac{dk^0}{2\pi} e^{-ik^0(t_1 - t_2)} S_1(k)$$
$$= \int \frac{dk^0}{2\pi i} e^{-ik^0(t_1 - t_2)} \frac{T}{k^0}\left(G_0^{R^2}(k) - G_0^{A^2}(k)\right).$$

Closing the contour in the lower (upper) halfplane for $t_1 - t_2$ larger (smaller) than zero, and calculating the residues at the double poles at $k^0 = \pm\omega_k - i\epsilon$ $(\pm\omega_k + i\epsilon)$ gives

$$S_1(\boldsymbol{k}, t_1 - t_2) = -\frac{T}{2\omega_k^4} \left(\omega_k(t_1 - t_2) \sin\omega_k(t_1 - t_2) + 2\cos\omega_k(t_1 - t_2)\right).$$

We remark that in this case it is crucial that S_0 is given by (C.4), in particular the k^0 dependence gives the correct contributions when calculating the residues at the poles.

We conclude that both methods give the same correct result. The standard thermal field theory approach can also be applied in the classical case.

Appendix D. Comparison between quantum and classical diagrams: the vertex function and setting sun self-energy

In this appendix we show that the classical diagrams (with the suitable matching relations) approximate the quantum expressions when the external momenta and frequencies are parametrically small compared to the temperature, of order $\sqrt{\bar{\lambda}}T$ for $\bar{\lambda} \to 0$. We

will first discuss the vertex function, which is primitively divergent only at one-loop order. It is illuminating to do the exercise, because it shows that the typical hard thermal loop structure is present, but not in leading order in the temperature. Then we discuss the setting sun contribution to the retarded self-energy, which is more involved.

The vertex function $\Gamma^{(1)}_{1112}(p)$ will be abbreviated to $\Gamma(p)$ in this appendix and we shall study $\Delta\Gamma(p) \equiv \Gamma(p) - \Gamma_{\rm cl}(p)$. To make the comparison easy, we introduce a momentum cutoff Λ to regulate the logarithmic divergence in the quantum diagram. We add a counterterm $C(\Lambda)$ with the finite parts chosen in such a way that the renormalized vertex function is the same as in the $\overline{\rm MS}$ scheme.

Using the result (8.2) for the quantum and classical ($n_k + \frac{1}{2} \to T/\omega_k$) vertex function, we find for the difference

$$\bar\lambda^{-2}\Delta\Gamma(p) = C(\Lambda) - \frac{1}{32\pi^2}\log\frac{\bar\mu^2}{\mu_T^2} + \int\frac{d^3k}{(2\pi)^3}\frac{1}{8\omega_k\omega_{k+p}}$$
$$\times\left[\left(n_k + n_{k+p} + 1 - \frac{T}{\omega_k} - \frac{T}{\omega_{k+p}}\right)\left(\frac{1}{p^0+\omega_k+\omega_{k+p}} - \frac{1}{p^0-\omega_k-\omega_{k+p}}\right)\right. \tag{D.1}$$
$$\left. + \left(n_{k+p} - n_k - \frac{T}{\omega_{k+p}} + \frac{T}{\omega_k}\right)\left(\frac{1}{p^0+\omega_k-\omega_{k+p}} - \frac{1}{p^0-\omega_k+\omega_{k+p}}\right)\right], \tag{D.2}$$

The second term on the first line comes from the matching relation between λ and $\bar\lambda$. It is convenient to rescale the variables as $\boldsymbol{k} = \boldsymbol{k}'T$, $\boldsymbol{p} = \sqrt{\bar\lambda}\,\boldsymbol{p}'T$, $p^0 = \sqrt{\bar\lambda}\,p'^0T$, $\bar m = \sqrt{\bar\lambda}\,\bar m'T$, to indicate the magnitude of the momenta, frequencies and the $\overline{\rm MS}$ mass parameter.

The first contribution (D.1) is the simplest. We take the limit $\bar\lambda \to 0$, which gives an expression that is infrared finite, because the apparent infrared danger cancels between the classical and the quantum contribution. The result is independent of p^μ. Isolating the logarithmic divergence by adding and subtracting the integral

$$\int_0^{\Lambda/T} dk'\frac{1}{k'+1} = \log\Lambda/T + \mathcal{O}(\Lambda^{-1}),$$

we find for the difference ($k' = |\boldsymbol{k}'|$)

$$\bar\lambda^{-2}\Delta\Gamma(p)_{(D.1)} = \frac{1}{8\pi^2}\int_0^\infty dk'\left[\frac{1}{k'}\left(\frac{1}{e^{k'}-1} + \tfrac{1}{2} - \frac{1}{k'}\right) - \frac{1}{2(k'+1)}\right] + \frac{1}{16\pi^2}\log\frac{\Lambda}{T}.$$

The integral is infrared and ultraviolet finite. The log divergence is cancelled with the counterterm $C(\Lambda)$. The $\log T$ term is cancelled by the matching relation, the other terms are order T^0 and hence subdominant.

The second contribution (D.2) can be calculated by using standard HTL methods [14]. Note that it is ultraviolet finite. We use

$$(\omega_{k+p} - \omega_k)/T = \sqrt{\bar{\lambda}}\,\hat{k}\cdot p' + \mathcal{O}(\bar{\lambda}),$$

$$n_{k+p} - n_k = \frac{\partial n'_{k'}}{\partial k'}\left[\omega_{k+p} - \omega_k\right] + \cdots, \qquad n'_{k'} = (\exp k' - 1)^{-1},$$

and similar for the difference of the classical distribution functions. The angular integrals are now decoupled from the k' integral, and the final result is ($p = |\boldsymbol{p}|$)

$$\bar{\lambda}^{-2}\Delta\Gamma(p)_{(D.2)} = \frac{1}{32\pi^2}\left(2 + \frac{p^0}{p}\log\frac{p-p^0}{p+p^0}\right).$$

This has the complicated momentum dependence of HTL expressions, but it is order T^0, hence subdominant at high T. From this we conclude that the leading order contribution in T to the quantum vertex function is given by the classical part. The reason for this is the following. If we leave out the vacuum part, and take the high-temperature limit *under* the integral sign, (which means that we replace the Bose distribution with the classical one), the resulting integral is still ultraviolet finite. Hence the integral is dominated by the low momenta, and the high-temperature limit under the integral sign gives the leading order behaviour (this is of course not true if the resulting integral becomes divergent, like in, e.g., the one-loop tadpole diagram).

Consider next the setting sun diagrams. We start with a discussion of $\Sigma^{\rm sun}_{R,\rm b}$, given in (7.4). Classically, there is no diagram like this. Since all the internal lines are retarded Green functions, there is no explicit temperature dependence. Therefore, this diagram represents a part of the vacuum contribution. Indeed, the sum of the vacuum part of $\Sigma^{\rm sun}_{R,\rm a}$ (given in (7.3)) with $\Sigma^{\rm sun}_{R,\rm b}$ gives the normal $T = 0$ expression. One is inclined to think that the vacuum contribution is order T^0 and hence subdominant at high T. However, because of the resummation there is an implicit T dependence. Because the diagram has dimension two, the momentum-independent part is proportional to $\bar{\lambda}^2 m^2$, which contains $\bar{\lambda}^3 T^2$. So there is a T^2 contribution, but fortunately it is suppressed by one power of the coupling constant. Therefore the vacuum contribution is subdominant after all, when we restrict ourselves to a small coupling constant.

The classical contribution $\Sigma^{\rm sun}_{R,\rm cl}$ is given in (7.9). A remarkable property of the classical expression is that the logarithmic divergence and the p^0 dependence are completely separated. This is possible because of the symmetry of the integrand. It turns out that the quantum diagram can also be written in such a way, which makes the comparison easier. After some rewriting, which is inspired by the Saclay method for calculating finite-temperature diagrams, the setting sun contribution in the quantum theory can be written as

$$\begin{aligned}\Sigma^{\rm sun}_R(p) &= \Sigma^{\rm sun}_{R,\rm a}(p) + \Sigma^{\rm sun}_{R,\rm b}(p)\\ &= -\tfrac{1}{2}\bar{\lambda}^2\sum_{\{\epsilon_i\}}\int d\Phi_{123}(\boldsymbol{p})\,\frac{1-e^{-\beta\epsilon_i\omega_{k_i}}}{p^0 + i\epsilon + \epsilon_i\omega_{k_i}}\prod_{j=1}^{3}(n_{k_j} + \bar{\epsilon}_j)\\ &= -\tfrac{1}{2}\bar{\lambda}^2\sum_{\{\epsilon_i\}}\int d\Phi_{123}(\boldsymbol{p})\,\frac{1-e^{-\beta\epsilon_i\omega_{k_i}}}{\epsilon_i\omega_{k_i}}\prod_{j=1}^{3}(n_{k_j} + \bar{\epsilon}_j) \qquad \text{(D.3)}\end{aligned}$$

$$+\tfrac{1}{2}\bar{\lambda}^2 p^0 \sum_{\{\epsilon_i\}} \int d\Phi_{123}(\boldsymbol{p}) \frac{1}{p^0 + i\epsilon + \epsilon_i \omega_{k_i}} \frac{1 - e^{-\beta \epsilon_i \omega_{k_i}}}{\epsilon_i \omega_{k_i}} \prod_{j=1}^{3} (n_{k_j} + \bar{\epsilon}_j), \tag{D.4}$$

where we used $\bar{\epsilon}_i = (\epsilon_i + 1)/2$. Similar as in the classical diagram, there is no p^0 dependence in the first term (D.3). All the p^0 dependence (and hence the specific problems related to time dependence) is contained in (D.4). When we restrict ourselves to time-independent correlation functions, only (D.3) is left over. Hence, this term is dealt by the dimensional reduction matching relations. In particular, when the mass vanishes, it develops an infrared divergence, which causes it to behave like $\bar{\lambda}^2 T^2 \log m/T$ for $\bar{\lambda} \to 0$ [19]. This term is matched (see (2.9)). Furthermore, the terms in the product that are linear in the Bose distribution give rise to a momentum-independent logarithmic ultraviolet subdivergence, proportional to T^2. This divergence cancels against a similar divergence in the second-order tadpole contribution to the retarded self-energy [18].

We now discuss the second term (D.4). Writing out the product gives terms that have three, two, one and zero Bose distribution functions. Only the last (vacuum) contribution is ultraviolet divergent. There is no subdivergence. (It would be proportional to p^0, but there is no such subdivergence [18]. The explicit p^0 factor cannot be cancelled by the vanishing of $\epsilon_i \omega_i$ in the denominator $p^0 + i\epsilon + \epsilon_i \omega_i$ because this can only cause a $\log p^0$ behaviour, not a $1/p^0$ behaviour.) Let's first look at the term with three Bose distributions. Taking the high-temperature limit under the integral sign (as in the vertex function case), results in a ultraviolet finite expression. Hence this expression gives the leading order behaviour. Furthermore we see that in this limit we recover in fact the second term in the classical expression (7.9). It now remains to show that the other terms (with two and one Bose distribution terms) are subdominant (here the high-temperature limit cannot be taken under the integral sign!). Rescaling the variables as in the vertex function case, gives a prefactor $\sqrt{\bar{\lambda}} T^2$. Furthermore there are no infrared divergences for $\bar{\lambda} \to 0$. Hence, although these terms are proportional to T^2, they are suppressed by a power of $\sqrt{\bar{\lambda}}$ (or $\sqrt{\bar{\lambda}} \log \bar{\lambda}$ in the case $\epsilon_i \omega_i$ vanishes in the denominator $p^0 + i\epsilon + \epsilon_i \omega_i$). For the real part of (D.4) we find a better result. Because it is even under $p^0 \to -p^0$, it is proportional to p^{0^2}, and hence after rescaling it is suppressed by a power of $\bar{\lambda}$, instead of $\sqrt{\bar{\lambda}}$.

The conclusion is that the leading part (at high T and small $\bar{\lambda}$) of the second term (D.4) is given by the corresponding classical expression.

The final result of this appendix is that the classical vertex and setting sun diagrams give the leading order quantum result, after matching. This matching is identical to the conventional dimensional reduction matching for time-independent quantities.

Appendix E. Relations between four-point functions

In this appendix we show that there is only one independent vertex function in ϕ^4 theory, by use of the relation with ϕ^3 theory.

The potential in a ϕ^3 theory becomes, after the transformation (3.4),

$$V(\phi) = \frac{g}{3!}\left(\phi_+^3 - \phi_-^3\right) = \frac{1}{2}g\phi_1^2\phi_2 + \frac{g}{4!}\phi_2^3.$$

The self-energies are again related through the KMS condition

$$\Sigma_F(p) = -i(n(p^0) + \tfrac{1}{2})\left(\Sigma_R(p) - \Sigma_A(p)\right).$$

The connection with the four-point function in ϕ^4 theory is straightforward

$$\Sigma_F^{(1)}(p) = -\Gamma_{1212}^{(1)}(p), \qquad \Sigma_R^{(1)}(p) = -\Gamma_{1112}^{(1)}(p).$$

Using these relations we find that only one vertex function is independent in the ϕ^4 theory.

References

[1] D.Yu. Grigoriev and V.A. Rubakov, Nucl. Phys. B 299 (1988) 67.
[2] D.Yu. Grigoriev, V.A. Rubakov and M.E. Shaposhnikov, Nucl. Phys. B 326 (1989) 737.
[3] J. Smit and W.H. Tang, Nucl. Phys. B (Proc. Suppl.) 42 (1995) 590;
[4] D. Bödeker, L. McLerran and A. Smilga, Phys. Rev. D 52 (1995) 4675.
[5] C. Greiner and B. Müller, Phys. Rev. D 55 (1997) 1026.
[6] P. Huet and D. T. Son, Phys. Lett. B 393 (1997) 94.
[7] G. Aarts and J. Smit, Phys. Lett. B 393 (1997) 395.
[8] W. Buchmüller and A. Jakovác, hep-ph/9705452.
[9] K. Farakos, K. Kajantie, K. Rummukainen and M. Shaposhnikov, Nucl. Phys. B 425 (1994) 67; B 442 (1995) 317.
[10] K. Kajantie, M. Laine, K. Rummukainen and M. Shaposhnikov, Nucl. Phys. B 458 (1996) 90; B 466 (1996) 189.
[11] A. Jakovác, Phys. Rev. D 53 (1996) 4538.
[12] J. I. Kapusta, Finite-Temperature Field Theory (Cambridge University Press, Cambridge, 1989).
[13] N.P. Landsman and Ch.G. van Weert, Phys. Rep. 145 (1987) 141.
[14] M. Le Bellac, Thermal Field Theory, (Cambridge University Press, Cambridge, 1996).
[15] A. Niégawa, Phys. Rev. D 40 (1989) 1199.
[16] T. S. Evans and A. C. Pearson, Phys. Rev. D 52 (1995) 4652.
[17] P. Aurenche and T. Becherrawy, Nucl. Phys. B 379 (1992) 259.
[18] N. Banerjee and S. Mallik, Phys. Rev. D 43 (1991) 3368.
[19] R.S. Parwani, Phys. Rev. D 45 (1992) 4695.
[20] E. Wang and U. Heinz, Phys. Rev. D 53 (1996) 899.
[21] E. Braaten and R. D. Pisarski, Nucl. Phys. B 337 (1990) 569; 339 (1990) 310.
[22] J. C. Taylor and S. M. H. Wong, Nucl. Phys. B 346 (1990) 115.
[23] P. Arnold, hep-ph/9701393.
[24] C. R. Hu and B. Müller, hep-ph/9611292.
[25] W.H. Tang and J. Smit, Nucl. Phys. B 482 (1996) 265.
[26] W.H. Tang and J. Smit, hep-lat/9702017.
[27] G.D. Moore and N.G. Turok, Phys. Rev. D 55 (1997) 6538.
[28] G. Parisi, Statistical Field Theory (Addison-Wesley, New York, 1988).